Composition of fluids in quartz: discrimination of magma pulses in a Caledonian granitoid

R. A. BATCHELOR

Department of Geography and Geology, University of St. Andrews, Fife, Scotland

D. C. ARMSTRONG

British Antarctic Survey, High Cross, Madingley Road, Cambridge

AND

M. MCDONALD

Department of Geography and Geology, University of St. Andrews, Fife, Scotland

Abstract

Fluids trapped inside fluid inclusions in quartz from the multiphase Starav monzogranite in Etive, Argyll, were extracted under vacuum and quantitative data for H_2O and CO_2 were obtained manometrically. Na and K were determined on an aqueous leach from the decrepitated grains. A bivariate diagram of H_2O/CO_2 versus Na/K discriminates between magma pulses and mirrors the whole-rock trace-element chemistry. This work shows that compositional variations of fluids in quartz from a weakly mineralised granitoid intrusion are sensitive indicators of its magmatic history and identify subtle changes in its mineralogical composition.

KEYWORDS: fluid composition, quartz, magma pulses, Caledonian granitoid.

Introduction

THE important role of fluids in mineralisation and petrogenesis has been recognised for a long time (Sorby, 1858) and information on their composition has until recently been obtained from optical studies of fluid inclusions (Roedder, 1972). Chemical analysis of the fluids trapped inside inclusions has been achieved both by crushing the sample under a solvent and analysing the leached cations (Roedder, 1958; Bottrell and Yardley, 1988) and by thermal decrepitation of the sample under vacuum followed by manometry and gas chromatography/mass spectrometry (Shepherd *et al.*, 1985). Most analytical studies on fluids have concentrated on mineralised rocks and investigations into the role of fluids in ore transport (Shepherd and Waters, 1984; Bottrell *et al.*, 1988; Wilkinson, 1990). This work describes the quantitative determination of H_2O, CO_2, Na and K in quartz and its application to the petrogenesis of a multiphase Caledonian granitoid which highlights a strong link between the composition of fluids in quartz and whole rock trace-element geochemistry.

Fluid extraction analysis

A prototype glass vacuum fluid extraction line modelled broadly on Shepherd *et al.* (1985) was linked in series with an oil pump and mercury diffusion pump which together reduced the internal pressure to 10^{-3} torr. A capacitance manometer was incorporated into the line to measure pressure of gases released after decrepitation of the sample. A cold finger trap containing liquid nitrogen froze out water, CO_2 and trace gases prior to manometric determination of cryogenic fractions or presentation to a linked gas chromatograph via a 4-way valve.

Quartz was separated from 15 samples representative of the four pulses of monzogranite. Each mineral sample was coarsely crushed and sieved, and the 1.0–0.5 mm (–16 + 30 mesh) fraction retained. Uncontaminated grains were hand-picked under a binocular microscope, washed in 4M HNO_3, rinsed ten times with deionised distilled water and dried at 110 °C. Approximately 0.1 g of clean quartz grains were accurately weighed, placed inside the vacuum line and degassed for 30 minutes at 110 °C. A decrepi-

Mineralogical Magazine, September 1992, Vol. 56, pp. 335–342
© Copyright the Mineralogical Society

tation temperature of 450 °C was chosen based on experimental runs on two vein quartz samples from mineralised areas in the Lake District and Nigeria. These showed evolved gas pressure maxima at 400 °C and 380 °C respectively. Above 480 °C, traces of carbonate begin to decompose and altered feldspar loses water (Behar and Pineau, 1979). Decrepitation of inclusions in quartz was deemed complete at 450 °C by Shepherd and Waters (1984). This chosen temperature was maintained for 10 minutes and volatile phases were isolated in a liquid-nitrogen-cooled trap. The residual pressure represented non-condensible phases. On removal of liquid nitrogen coolant, the pressure rose rapidly then stabilised after 30 seconds and remained constant for 10 seconds. This value represented CO_2 (plus traces of other condensible phases). Water was not catalytically converted to H_2 but was released by rapid warming of the cold trap by a hot air blower which minimised the internal surface tension effects of water on glass, and produced a transient maximum pressure reading which was recorded.

A larger aliquot (~0.4 g) of quartz (RB101) was treated in a similar manner, but the non-aqueous condensible phases were sent direct to a gas chromatograph incorporating a 6′ × ⅛″ glass column, filled with 'Porapak Q' 80–100 mesh, which was connected to a thermal conductivity detector. Helium flow was 25 mL/min and the oven temperature was 30 °C isothermal. The column was calibrated using a standard gas mixture. The output indicated that CO_2 consituted >99% of this fraction. On this evidence, all manometric readings taken 40 seconds after removal of liquid nitrogen cooling were assumed to represent CO_2.

The decrepitated grains were retrieved and leached for 2 hours in deionised distilled water heated to 80 °C and acidified with 0.5 mL 3M HNO_3. The resulting solution was analysed for Na and K by atomic absorption spectrophotometry.

A quartz sample (No. CF-77-77A) from Carrock Fell, Lake District, previously analysed by T. J. Shepherd (pers. comm.) was subjected to the same procedure and the results obtained are listed in Table 1. Reproducibility was determined on replicate runs of two vein quartz samples (Table 2).

TABLE 1 Data for Carrock Fell quartz, CF-77-77A.

	N.C.	CO_2	H_2O	H_2O/CO_2
a	0.3	1.47	74.7	51
b	0.4	1.5	72.6	48
c	0.4	1.4	75.3	53
d	0.35	1.48	71.3	48

a = Data of T.J.Shepherd (pers. comm.).
b,c,d = Data obtained by the technique described in this paper.
N.C. = Non-condensible phases.
N.C., CO_2, and H_2O data expressed in μmole per gram of quartz.

Microthermometry

Microthermometric measurements were carried out on individual inclusions from four rock samples representing the four different magma pulses prepared as free-standing, doubly-polished wafers following the method of Shepherd *et al.* (1985). Only fluid inclusions in quartz were studied (Fig. 1*a–d*).

At room temperature most of the inclusions are

TABLE 2 Reproducibility data for fluids in quartz

	N.C.	CO_2	H_2O
	BRAZIL QUARTZ		
	0.54	3.9	5.8
	0.60	3.8	5.6
	0.50	3.8	5.1
	0.52	3.8	5.6
Mean ± 1 S.D.	0.54±0.04	3.8±0.05	5.5±0.3
	PEGMATITE QUARTZ RB101A		
	0.22	1.84	93.4
	0.12	1.79	93.3
	0.10	1.93	97.8
	0.18	1.90	94.0
Mean ± 1 S.D.	0.15±0.06	1.86±0.06	94.6±1.9

N.C. = Non-condensible phases.
Values for N.C., CO_2 and H_2O expressed in μmole per gram of quartz.
1 S.D. = One standard deviation.

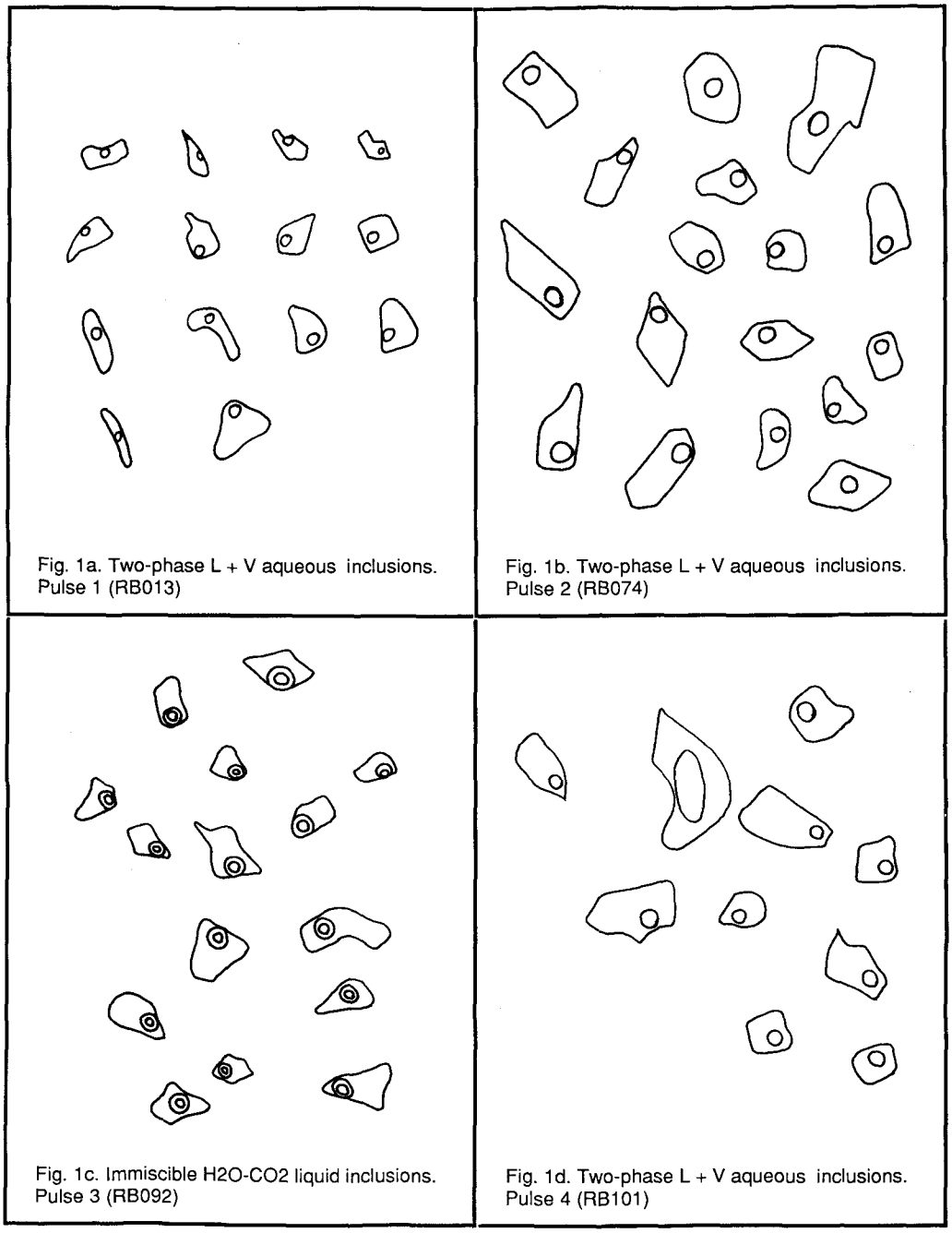

Fig. 1a. Two-phase L + V aqueous inclusions. Pulse 1 (RB013)

Fig. 1b. Two-phase L + V aqueous inclusions. Pulse 2 (RB074)

Fig. 1c. Immiscible H2O-CO2 liquid inclusions. Pulse 3 (RB092)

Fig. 1d. Two-phase L + V aqueous inclusions. Pulse 4 (RB101)

FIG. 1. Sketch of fluid inclusions representative of each magma pulse.

aqueous two-phase types containing both a liquid and vapour phase. These two-phase aqueous inclusions are most commonly equant to ellipsoidal in shape although some show evidence of post-entrapment necking and are orientated along fracture planes. They show considerable

variations in size from below the resolution of the microscope up to 20 μm and are present in all wafers studied. CO_2–water immiscible liquid inclusions only occur in specimen RB092 which represents pulse 3. These 'bubble in bubble' inclusions consist of an aqueous liquid surrounding a CO_2-rich one, which in turn surrounds a CO_2-rich vapour bubble. The CO_2-rich vapour bubble is agitated at room temperature because the CO_2-rich phase of the inclusion is close to homogenisation. These inclusions are generally about 10 μm in diameter and predominate over the two-phase aqueous inclusions. A few monophase liquid and monophase vapour inclusions are also present in all samples.

A Linkam TH600 heating/freezing stage mounted on an Olympus BH-2 polarizing microscope and connected to a Linkam PR600 programmable unit with digital temperature display was used for the microthemometric study (Shepherd, 1981). All microthermometric measurements on all inclusion types were made during the heating (melting) cycle to allow for the effects of supercooling, and measurements were made at sub-ambient temperature first, followed by a systematic progression to high temperatures.

All the aqueous inclusions measured from all four magma pulses have temperature of first ice melting (Tfm_{ice}) above −30 °C (Table 3) and consideration of eutectic temperatures for salt–water systems suggests a Na–K–Cl dominated system. However, inclusions with Tfm_{ice} below −24 °C may also contain a Ca or Mg component (Borisenko, 1977; Crawford, 1981).

Aqueous inclusions from magma pulse 1 show a mixture of equant and 'necked' inclusions. They have temperature of last ice melting (Tm_{ice}) ranging from −1.7 to −6.3 °C. Assuming 1:1 KCl:NaCl, these values yield salinity estimates between 3.1 and 11.3 wt.% salt (Shepherd *et al.*, 1985, p. 73). Aqueous inclusions from magma pulse 2 have Tm_{ice} from +0.2 to −5.9 °C which corresponds to salinites of 0 to 11.1 wt.% The wafer representing magma pulse 3 contains few aqueous inclusions and only one measurement was made on this type. It gave a Tfm_{ice} value of −6.3 °C which indicates a salinity of 11.3 wt.%. Aqueous inclusions from magma pulse 4 have Tm_{ice} ranging from to +1.8 to −4.5 °C, which corresponds to salinites of 0 to 7.4 wt.% (Table 3).

Without exception, all the aqueous inclusions showed final homogenisation into the liquid state. Results of total homogenisation temperature (Th_{tot}) measurements on the aqueous inclusions from all magma pulses are similar. Th_{tot} for pulse 1 inclusions range from +206 to +276 °C. Pulse 2 inclusions have Th_{tot} from +125 to +166 °C. The single value for the aqueous inclusion in pulse 3 gives +189 °C. Pulse 4 yield values ranging from +147 to +249 °C.

In considering the CO_2–water immiscible inclusions from magma pulse 3, the final melting temperature of solid CO_2 (Tm_{CO_2}) is a measure of the purity of the phase. Pure CO_2 melts at −56.6 °C, the triple point of CO_2, and addition of other gases such as CH_4, N_2, H_2S and SO_2 results in a depression of this triple point. All the immiscible liquid inclusions measured have CO_2 fusion temperatures in the range −55.9 to −59.6 °C. Allowing for the fact that the Linkam stage is accurate to ±1 °C at these temperatures they are not significantly different from the fusion temperture of CO_2 and confirm that the phase is pure CO_2. At ambient temperatures the aqueous

TABLE 3 Summary of microthermometric data.

	Range	Mean	n
RB013 - PULSE 1			
Two-phase (liquid + vapour) aqueous inclusions			
Tfm_{ice}	−29.0		1
Tm_{ice}	−1.7 to −6.3	−4.8	6
Salinity	3.1 to 11.3 wt%	8.4 wt%	
Th_{tot}	206 to 276	233	18
RB074 - PULSE 2			
Two-phase (liquid + vapour) aqueous inclusions			
Tfm_{ice}	−18.8 to −24.2	−21.1	3
Tm_{ice}	0.2 to −5.9	−3.8	14
Salinity	0 to 11.1 wt%	6.5 wt%	
Th_{tot}	125 to 166	152	7
RB092 - PULSE 3			
Water - Carbon dioxide immiscible inclusions			
Tm_{CO2}	−55.9 to −56.9	−56.3	5
Tm_{clath}	5.5 to 6.9	6.2	6
Salinity	6.1 to 8.4 wt%	7.2 wt%	
Th_{CO2}	27.3 to 30.0	28.3	9
Density CO_2	0.58 to 0.68	0.65 g/cm^3	
Th_{tot} + T_{dec}	231 to 372	299	10
Two-phase (liquid + vapour) aqueous inclusions			
Tfm_{ice}	−15.4		1
Tm_{ice}	−6.3		1
Salinity	11.3 wt%		
Th_{tot}	189		1
RB101 - PULSE 4			
Two-phase (liquid + vapour) aqueous inclusions			
Tfm_{ice}	−30.1		1
Tm_{ice}	1.8 to −4.5	−1.8	9
Salinity	0 to 7.4 wt%	3.7 wt%	
Th_{tot}	147 to 249	200	8

All temperatures expressed in °C.
n = number of observations

fluid and CO_2 phases are completely immiscible but on cooling there is strong interaction between them to form gas hydrates ('clathrates') which disturb the behaviour of the remaining aqueous and non-aqueous phases. The residual aqueous solution will be more saline than the original and any estimate of salinity based on the depression of the freezing point of ice will give an erroneously high value. As the clathrate fusion temperature is also a function of salinity the temperature of last clathrate melting (Tm_{clath}) can give an estimate of the salinity (Collins, 1979). Tm_{clath} for the immiscible liquid inclusions range from +5.5 to −6.9 °C giving a salinity estimate of 6.1 to 8.4 wt.% salt. All CO_2 liquid and vapour homogenisations observed in this study were into the liquid phase. From measured CO_2 homogenisation (Th_{CO_2}) values (+27.3 to +30.0 °C) the density of the CO_2 phase is calculated to be 0.58 to 0.68 g/cm^3 (Shepherd *et al.*, 1985, p. 115).

Owing to their high CO_2 content the immiscible liquid inclusions develop high internal pressures on heating (Burruss, 1981*a*,*b*) and even when heated at very slow rates some decrepitated below their total homogenisation temperature. In such cases the decrepitation temperature (T_{dec}) can be considered to be a low estimate of the homogenisation temperature (Th_{tot}). Total homogenisation temperatures (including temperatures of decrepitation) for the immiscible liquid inclusions range from +231 to +372 °C, average +299 °C (Table 3).

Results and discussion

The compositions of fluids extracted from the quartz are shown in Table 4.

A geochemical study of the Etive granitoid complex (Fig. 2) recognised that the Starav monzogranite facies was composed of four nested pulses (Fig 3,4) (Batchelor, 1987). When data for μmole H_2O/CO_2 and atomic ratio Na/K were plotted it became apparent that the variation in fluid composition mirrored the whole-rock trace-element pattern in discriminating between three out of four pulses (Fig. 5).

Moving from pulse 1 to pulse 2 shows a general relative increase in CO_2 with increasing Na/K. Pulse 3 is a conspicuous in having the highest relative CO_2 content and shows an overall increase in Na/K with decreasing H_2O/CO_2. Pulse 4 shows a relative increase in CO_2 from the outer margin to its centre, culminating in the CO_2-rich pegmatite. Whereas Na/K values increase with a relative increase in CO_2 in pulses 2 and 3, this ratio falls within pulse 4 towards the centre. The appearance of monazite in this pulse was noted by Barritt (1983). The distribution of U within pulse 4 is bimodal, averaging 3.08 ppm in the outer facies and 7.89 ppm in the inner facies. The inner facies contains the highest levels of U in the Etive pluton (6.1 to 11.6 ppm) compared with a mean value of 2.7 ppm in the rest of the pluton (Barritt, 1983). The inner facies is also host to disseminated molybdenite mineralisation (Haslam and

TABLE 4 Composition of fluids in quartz, Starav monzogranite, Etive.

Sample	N.C.	CO_2	H_2O	H_2O/CO_2	Na/K	CO_2 mole%
Pulse 1						
RB013	0.13	0.20	31.0	155	2.12	0.60
RB065	0.15	0.13	25.5	196	2.21	0.80
Pulse 2						
RB015	0.08	0.30	37.3	124	4.70	0.80
RB017	0.14	0.14	25.9	185	2.20	0.54
RB074	0.10	0.22	35.5	161	3.02	0.62
RB080	0.15	0.17	27.0	159	2.12	0.63
RB032	0.12	0.20	26.0	130	5.24	0.76
Pulse 3						
RB095	0.22	0.57	38.2	67	2.60	1.48
RB096	0.25	0.46	24.1	52	3.10	1.89
RB014	0.10	0.57	27.8	49	3.96	2.04
RB092	0.14	0.60	24.7	41	4.70	2.41
Pulse 4						
RB034	0.09	0.12	26.4	220	1.82	0.45
RB093	0.10	0.16	32.8	205	2.55	0.48
RB101	0.08	0.20	21.8	109	0.78	0.91
RB106	0.12	0.21	17.4	83	0.45	1.19
Pegmatite RB101A (mean of 4)	0.15	1.86	94.6	50	7.25	1.96

N.C. = Non-condensible phases.
N.C., CO_2 and H_2O data expressed in μmole per gram of quartz.
Na/K expressed as atomic ratio.

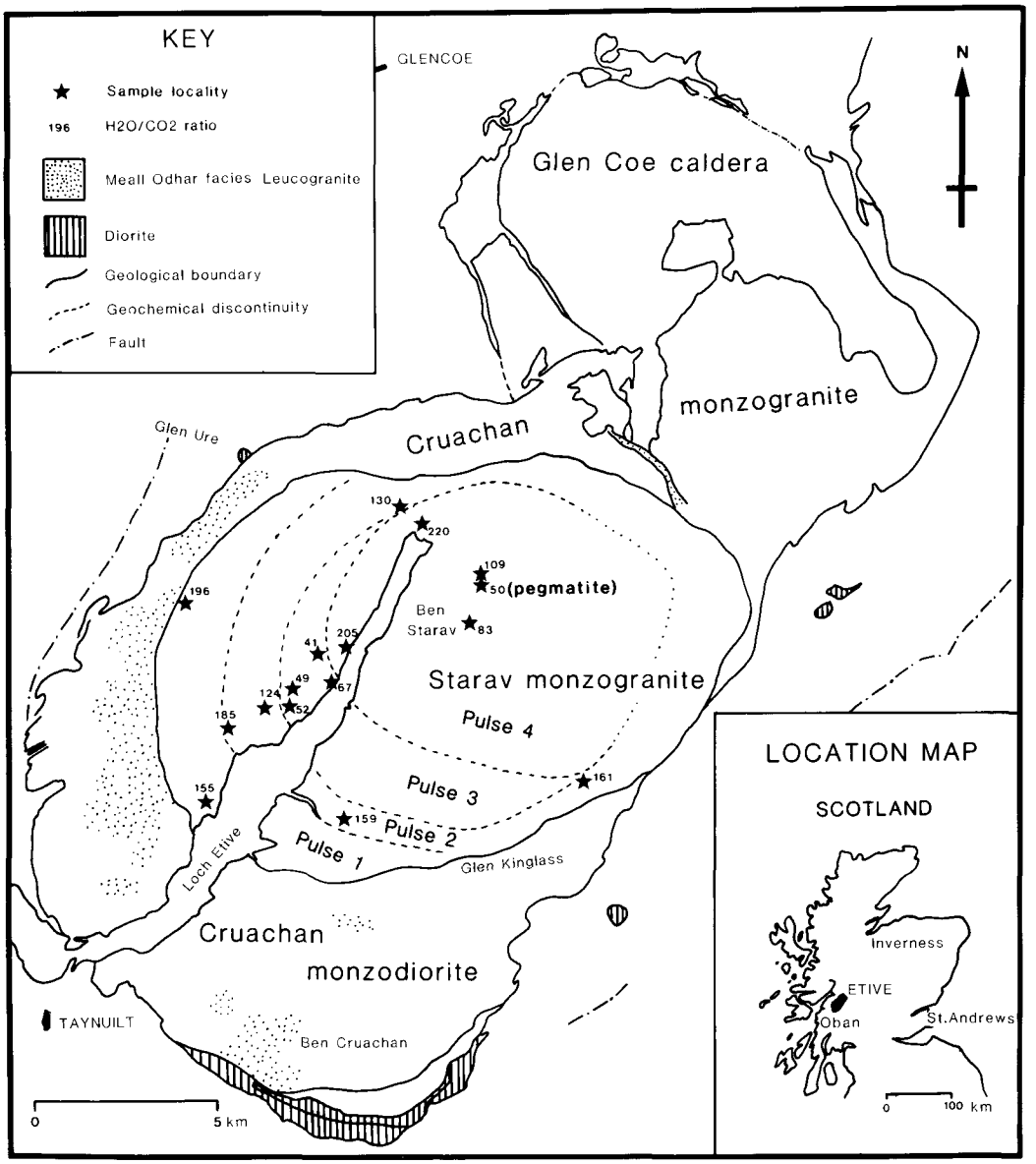

FIG. 2. Outline geological map of the Etive Granitoid Complex, Argyll, showing localities of samples used in this study. The H_2O/CO_2 data, expressed as μmole/g, are superimposed.

Cameron, 1985). This mineralised facies is characterized by low Na/K and low H_2O/CO_2.

The two phase (liquid + vapour) aqueous inclusions from all four magma pulses have low salinites (means: 3.7% to 11.3%) and temperatures of homogenisation with means ranging from 152 °C to 233 °C, suggesting that a moderate temperature, low salinity aqueous fluid was present in all magma pulses. The fact that most inclusions are equant or ellipsoidal in shape strongly suggests they are of primary origin and therefore that their composition is unique to each pulse. Since the variation in fluid composition discriminates between pulses this suggests that any late-stage fluid overprint was insufficient to mask the primary fluid signature. It should also be noted that in pulse 3 the order of samples which define the fluid compositional trend is mirrored

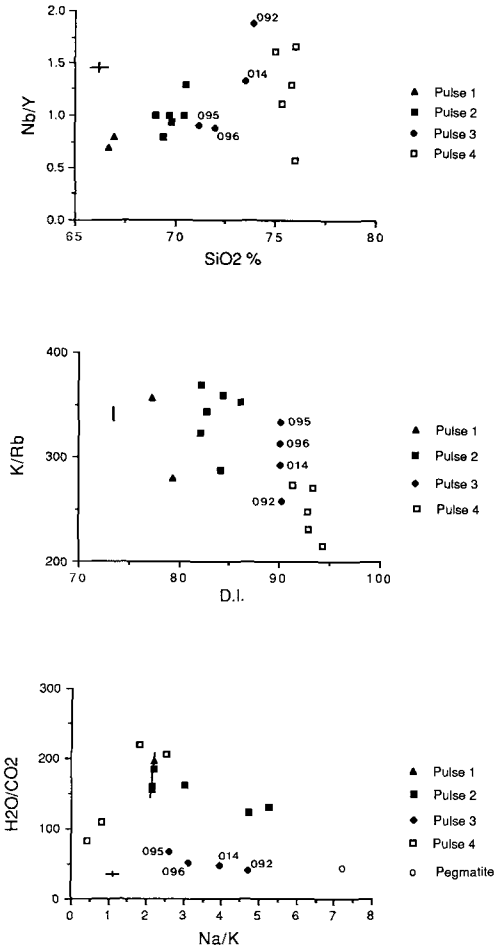

FIGS, 3–5. FIG. 3. (*top*) Whole-rock geochemistry bivariate diagram, Nb/Y *vs.* SiO_2% (error bars, ± S.D., shown upper left). FIG. 4. (*centre*) Whole-rock geochemistry bivariate diagram, K/Rb vs. D.I. (Differentiation Index; Thornton and Tuttle, 1960) (error bar, ± 1 S.D., shown upper left). FIG. 5. (*bottom*) Variation diagram for H_2O/CO_2 (μmole/g) vs. Na/K (atomic ratio). The tie line connects Pulse 1 samples (error bars, ±1 S.D., shown lower left).

exactly in the bulk rock K/Rb and Nb/Y values. The presence of abundant CO_2–water immiscible liquid inclusions in material from magma pulse 3 suggests that a different source was involved. In agreement with the bulk analytical work the presence of CO_2 and high temperatures of homogenisation from these inclusions supports the interpretation that pulse 3 represents an influx of CO_2-rich magma.

The range of Na/K atomic ratio values for the Etive samples, excluding the pegmatite (0.45–5.24, mean 2.77) fall within the span of values quoted for magmatic fluids by Wilkinson (1990) (3.95 atomic ratio) and Hansteen and Lustenhouwer (1990) (0.74 atomic ratio). In contrast, Wilkinson (op.cit.) notes that low-temperature retrogressive metamorphic fluids in Cornubian granites show Na/K values ranging from 9.7 to 18.3 atomic ratio. These data strengthen the evidence that the Etive fluids trapped in quartz are primarily magmatic. The quartz–microcline pegmatite sample (RB101A) which occurs within pulse 4 contains higher H_2O and CO_2 than its host and has a Na/K value of 7.25 (atomic ratio). Thermometric data yields Th_{tot} 166–200 °C and a low salinity of 3% (J. A. Kinnaird, pers. comm.) which are similar to the host granite. However, the higher concentration of volatiles and relatively higher Na are consistent with the formation of the pegmatite by slow cooling of residual melt.

These results show that a combination of H_2O, CO_2, Na and K data from fluids extracted from fluid inclusions in quartz from a granitoid, supported by thermometric data, can highlight the existence of separate magma pulses and complement whole-rock geochemical data in fingerprinting granitoid facies. They also point to the combination of low H_2O/CO_2 and low Na/K values as indicative of U and Mo mineralisation.

Acknowledgements

The establishment of a fluid extraction line was instigated by Dr. P. Bowden and it was designed and built by Professor T. R. Blackburn (St. Andrews College, Laurinburg, U.S.A.) in collaboration with Dr. T. J. Shepherd (BGS), R. A. B. and Mr. C. Smith (Dept. of Chemistry). Dr. J. A. Kinnaird is thanked for useful discussion and an anonymous referee for making constructive criticism of an earlier draft. D. C. A. is grateful to B.A.S. for leave to perform the thermometric work and M. M. thanks M. A. Bells for support.

References

Barritt, S. D. (1983) *The controls of radioelement distribution in the Etive and Cairngorm granites: implications for heat production.* Open University, Ph.D. thesis (unpubl.)

Batchelor, R. A. (1987) Geochemical and petrological characteristics of the Etive granitoid complex, Argyll. *Scott. J. Geol.*, **23**, 227–49.

Behar, F. and Pineau, F. (1979) Analyse de CO_2, H_2O, hydrocarbures des inclusions fluides par chromatographie en phase gazeuze: application aux fentes alpines et aux roches metamorphiques. *Bull. Mineral.*, **102**, 611–21.

Borisenko, A. S. (1977) Study of the salt composition of solutions in gas-liquid inclusions in minerals by the cryometric method. *Soviet Geology and Geographics*, **18**, 11–19.

Bottrell, S. H. and Yardley, B. W. D. (1988) The composition of a primary granite-derived ore fluid from SW England determined by fluid inclusion analysis. *Geochim. Cosmochim. Acta,* **52**, 585–8.

—— Shepherd, T. J., Yardley, B. W. D., and Dubessy, J. (1988) A fluid inclusion model for the genesis of the ores of the Dolgellau Gold Belt, North Wales. *J. Geol. Soc. Lond.,* **145**, 139–45.

Burruss, R. C. (1981*a*) Analysis of phase equilibria in C–O–H–S fluid inclusions. In *Short Course in Fluid Inclusions: Applications to Petrology.* (L. S. Hollister and M. L. Crawford, eds.), *Min. Assoc. Can. Short Course Handbook,* **6**, 39–74.

—— (1981*b*) Analysis of fluid inclusions: phase equilibria at constant volume. *Amer. J. Sci.,* **281**, 1104–26.

Collins, P. L. F. (1979) Gas hydrates in CO_2-bearing fluid inclusions and the use of freezing data for estimation of salinity. *Econ. Geol.,* **74**, 1435–44.

Crawford, M. L. (1981) Phase equilibria in aqueous fluid inclusions. In: *Short Course in Fluid Inclusions: Applications to Petrology* (L. S. Hollister and M. L. Crawford, eds.), *Min. Assoc. Can. Short Course Handbook,* **6**, 75–100.

Hansteen, T. H. and Lustenhouwer, W. J. (1990) Silicate melt inclusions from a mildly peralkaline granite in the Oslo paleorift, Norway. *Mineral. Mag.,* **54**, 195–205.

Haslam, H. W. and Cameron, D. G. (1985) Disseminated molybdenum mineralisation in the Etive plutonic complex in the western Highlands of Scotland. *Mineral. Reconn. Prog. Rep. B.G.S.,* No. 76.

Roedder, E. (1958) Technique for the extraction and partial chemical analysis of fluid-filled inclusions from minerals. *Econ. Geol.,* **53**, 235–69.

—— (1972) Compositions of fluid inclusions. *U.S. Geol. Surv. Prof. Paper,* **440-J**.

Shepherd, T. J. (1981) Temperature–programmable heating-freezing stage for microthermometric analysis of fluid inclusions. *Econ. Geol.,* **76**, 1244–7.

—— and Waters, P. (1984) Fluid inclusion gas studies, Carrock Fell Tungsten Deposit, England: Implications for regional exploration. *Mineral. Deposita,* **19**, 304–14.

—— Rankin, A. H., and Alderton, D. H. M. (1985) *A Practical Guide to Fluid Inclusion Studies.* Blackie, Glasgow.

Sorby, H. C. (1858) On the microscopic structure of crystals, indicating the origin of minerals and rocks. *Quart. J. Geol. Soc.,* **14**, 453–500.

Thornton, C. P. and Tuttle, O. F. (1960) Chemistry of igneous rocks. 1. Differentiation Index. *Amer. J. Sci.,* **258**, 664–84.

Wilkinson, J. J. (1990) The role of metamorphic fluids in the development of the Cornubian orefield: fluid inclusion evidence from south Cornwall. *Mineral. Mag.,* **54**, 219–30.

[*Manuscript received 19 May 1988: revised 13 September 1991*]